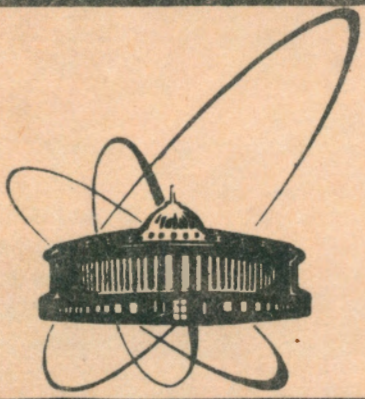

сообщения
объединенного
института
ядерных
исследований
дубна

E1-92-174

A.V.Daniel*, V.G.Lyapin*, I.O.Tsvetkov*,
V.I.Yurevich, R.M.Yakovlev*

NEUTRON PRODUCTION IN LEAD TARGETS BY HIGH-ENERGY LIGHT-MASS HEAVY IONS

*V.G.Khlopin Radium Institute, Saint Petersburg

1992

INTRODUCTION

A problem of forming medium- and high-energy nuclear data file is an important task at present. A successful development of a lot of applications in science and practice depends on this problem. With reference of neutron data they have the most cost. But nowadays there is very poor experimental nuclear data set at the energy region above 100 MeV/nucleon. This prevents to produce the evaluated experimental data library. But recently the attempt to widen the ENDF/B-VI library to 1 GeV was undertaken by Pearlstein[1]. However, a comparison of these results with theoretical predictions showed the unaccountable discrepancy between the experiment and the theory[2-4]. So an accumulation of experimental information is the main task at present.

The systematic investigations of neutron production in thin and thick lead targets was performed by groups from KfK[5-7] and LANL[8-10] in the energy region of incident protons 100-1100 MeV. The proton spectra were also measured by KfK group. The beam of protons with energy above 1 GeV was used in the measurements of cross-sections of high-energy neutron and proton production by ITEP group[11,12]. But there are no any systematic investigations of neutron production in lead targets by relativistic heavy ions besides of the results of Cecil et al.[13] obtained with 640 and 710 MeV alpha-particles.

During last years we measured the neutron and charged particle energy distributions for thin and thick lead targets bombarded by 2.0 GeV and 2.55 GeV protons and d, α, ^{6}Li and ^{12}C ions with the energy of 1 GeV per nucleon. The main our purpose was to obtain the neutron data for the accelerator-based neutron spallation sources design. This research was supported by μCF program.

EXPERIMENTAL METHOD

The measurements were performed by the time-of-flight technique on our hadron spectrometer based on the JINR synchrophasotron. The schematic drawing of the target-detectors arrangement at the JINR synchrophasotron is given in fig.1. The block diagram of the electronics used in the TOF-spectrometer is given in fig.2. A neutron emission was studied at three different angles (at present after the reconstruction the spectrometer has four identical arms) using three types of detectors with stylben crystals ϕ40x10 mm^3 and ϕ50x50 mm^3 and plastic scintillators ϕ120x200 mm^3. This detector set overlapped very wide energy region from 0.2 MeV to about the beam energy containing more than 95% of all emitted neutrons. Using one of them we could study all stages of neutron emission – cascade,

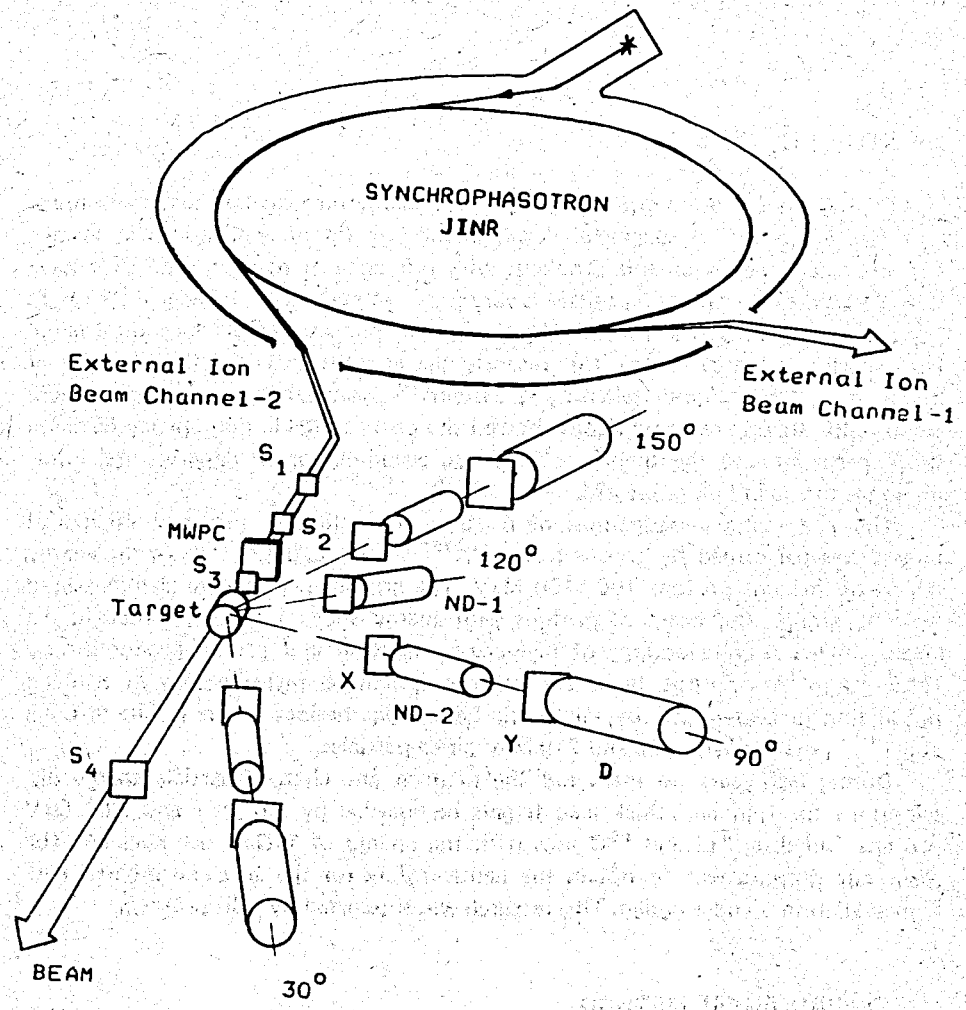

Fig.1. Schematic drawing of the target-detectors arrangement at the JINR synchrophasotron: S1-S4 — beam counters and X, Y — veto-counters with thin plastic scintillators, ND-1 — detector with stylben $\phi 40 \times 10$ mm^3, ND-2 - detector with stylben $\phi 50 \times 50$ mm^3, D — detector with plastic scintillator $\phi 120 \times 200$ mm^3.

pre-equilibrium and equilibrium. Thin 3 or 5 mm plastic scintillators as veto-counters for charged particles were placed in front of all detectors. For stylben detectors n-γ pulse-shape discrimination was employed. A separation of neutron- and gamma-events was performed in a stage of off-line data analysis. As example, two

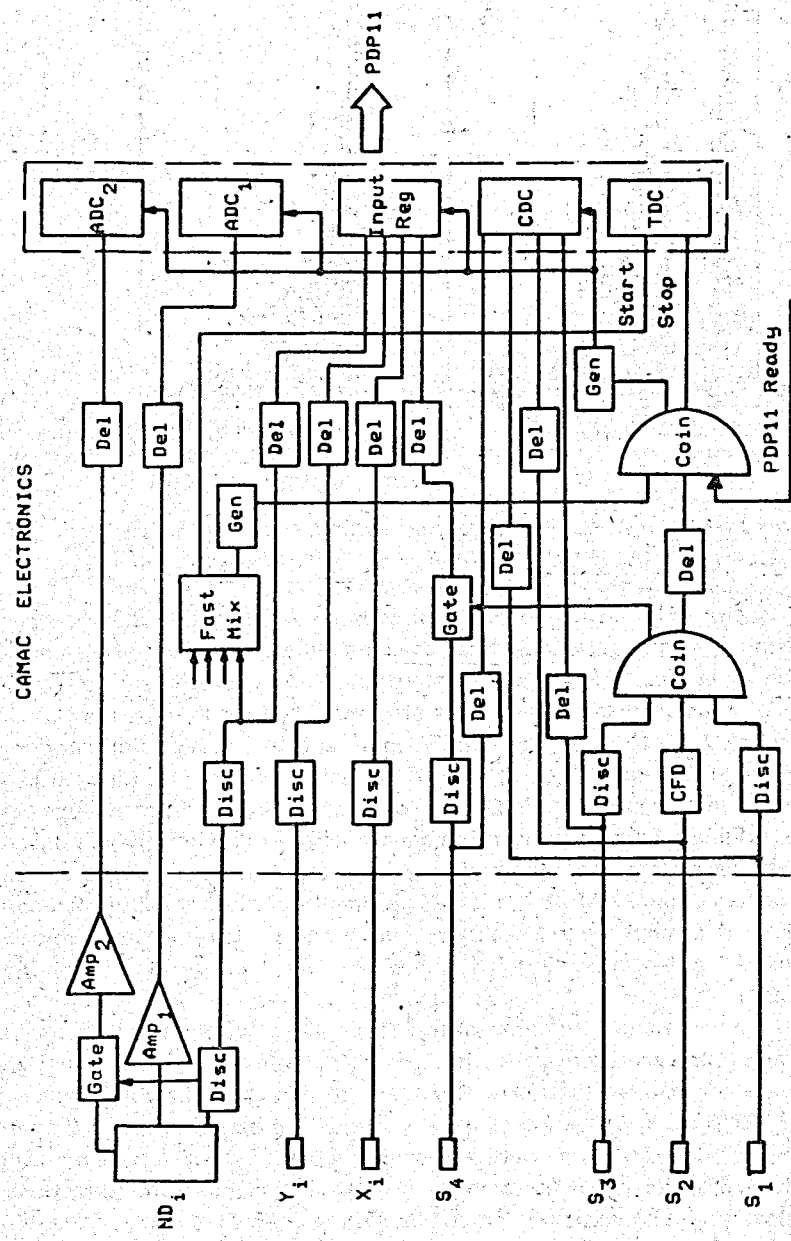

Fig.2. Block diagram of electronics used in the time-of-flight spectrometer. The abbreviations are as follows: Disc — discriminator, Amp — linear amplifier, Del — delay, CFD — constant fraction discriminator, Coin — coincidence, Gen — generator, ADC — analog-to-digital converter, Input Reg — input register, CDC — charge-to-digital converter, TDC — time-to-digital converter.

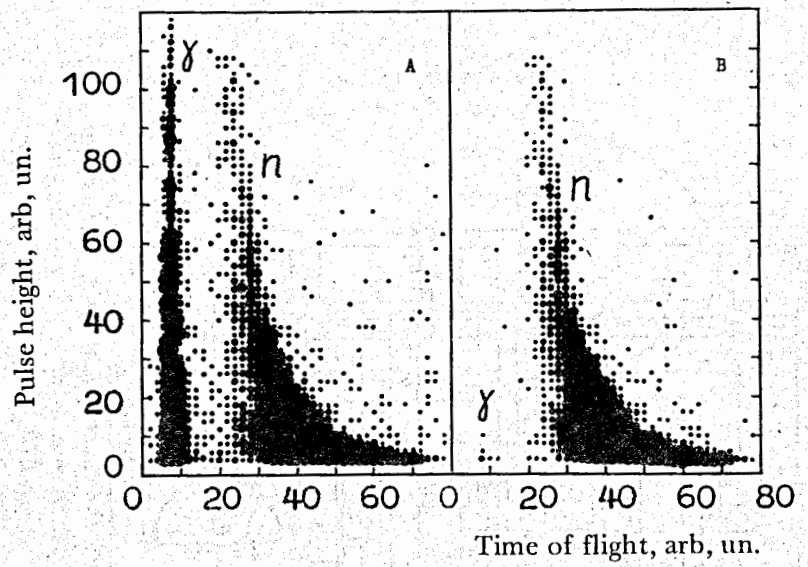

Fig.3. Two time-of-flight spectra measured with the fast ionization chamber with a layer of ^{252}Cf: (A) — without and (B) — with n-γ discrimination.

time-of-flight spectra (without and with n-γ discrimination) measured using the fast ionization chamber with a layer of ^{252}Cf as the source of neutrons and gamma-quanta are shown in fig. 3. Many efforts were undertaken to accurate determine the efficiency of neutron detectors[14]. The efficiency data for the detectors based on stylben crystals ϕ40x10 mm^3 and ϕ50x50 mm^3 and the plastic scintillator for values of threshold 0.1, 1 and 30 MeV, respectively, are given in fig. 4. Charged particle spectra were measured with X-Y-D detector telescopes. The different types of particles were off-line separated using t-E (time-of-flight — pulse height) plot analysis. In fig. 5 the example of t-E plot is shown for charged particles emitted at 90° from thick lead target by 1 GeV·A ^6Li ions. The time resolution was about 0.5 and 1 ns/m (FWHM of prompt gamma-peak) for plastic and stylben detectors, respectively. The typical flight paths were 0.7, 1.3 and 2.0 m for the detectors ND-1, ND-2 and D respectively.

The ion beam had a pulse structure that consisted of macropulse that were about 350 ms long and following through 9 s with about 10^5 ion/macropulse. Within each macropulse were micropulses that were about 20 ns wide and following one after another through 300 ns. The position and the profile of the beam in front of the target was monitored by means of multiwire proportional chamber (MWPC). Beam size was typically 20 mm (FWHM) both in the vertical and horizontal directions.

Data accumulation was accomplished employing the on-line computer. The experimental method and the setup were described in detail in ref.[15]. The list of measurements performed for three last years is given in the table.

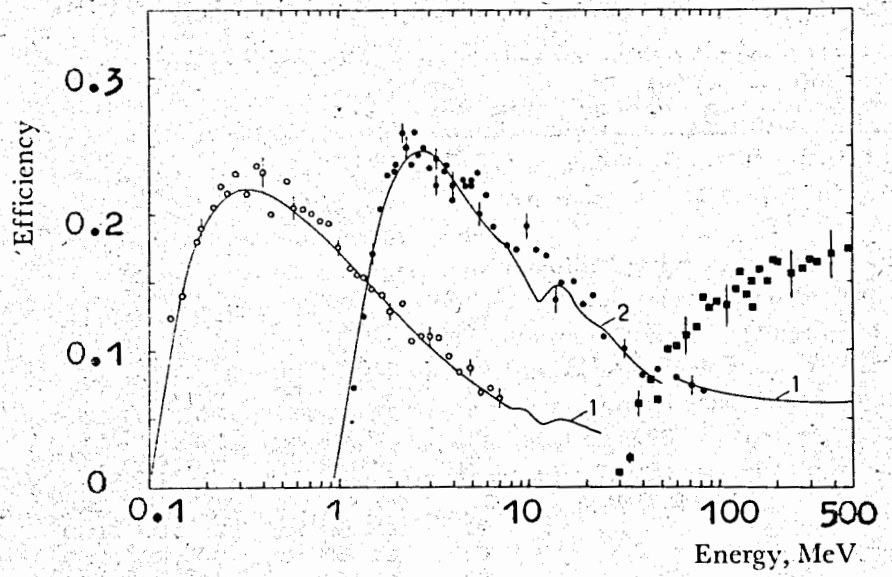

Fig.4. Efficiency for three types of neutron detectors with values of thresholds 0.1 MeV (stylben ϕ40x10 mm^3), 1 MeV (stylben ϕ50x50 mm^3) and 30 MeV (plastic scintillator ϕ120x200 mm^3). The points — experimental results, the curves — results of calculations.

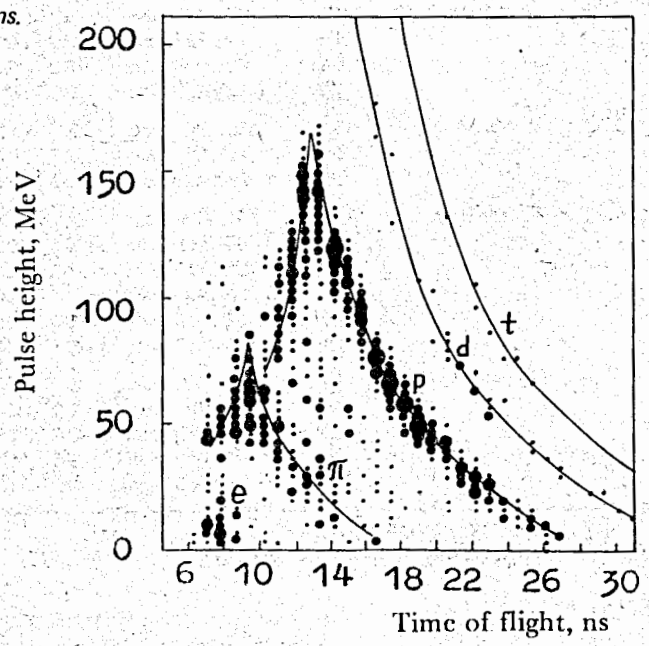

Fig.5. t-E plot for charged particles measured at 90° on 1 GeV·A ^6Li ion beam with lead target 8x8x8 cm^3.

Table. Our last time-of-flight measurements (beams, targets, angles)

Number of experiment	Beam ion	energy	Target nucleus*	size**	Angle
1	^{6}Li	1 GeV A	C	23.3 mm	90°
			C	100 mm	90°
			Pb	8x8x8 cm	90°
			Pb	ϕ20x20 cm	90°
2	p	2.55 GeV	Al	ϕ20x20 cm	90°
			Pb	8x8x8 cm	90°
			Pb	ϕ20x20 cm	30°,90°,150°
3	p	2.00 GeV	Be	8x8x4 cm	30°,90°
			Al	17.32 mm	30°,90°,150°
			Cu	11.43 mm	30°,90°,150°
			Pb	6.93 mm	30°,90°,150°
			Pb	8x8x8 cm	30°,90°,150°
4	^{12}C	2 GeV A	C	30.60 mm	30°,90°,150°
			Al	23.09 mm	30°,90°,150°
			Cu	11.55 mm	30°,90°,150°
			Pb	13.86 mm	30°,90°,150°
5	d	1 GeV A	Pb	6.93 mm	30°,90°,150°
			Pb	8x8x8 cm	30°,90°,150°
			Pb	ϕ20x20 cm	30°,90°,150°
6	^{4}He	1 GeV A	C	31.18 mm	30°,90°,150°
			Pb	6.93 mm	30°,90°,150°
			Pb	8x8x8 cm	30°,90°,150°
			Pb	ϕ20x20 cm	30°,90°,150°
7	^{12}C	1 GeV A	Cu	15.60 mm	30°,60°,90°
			Pb	12.00 mm	30°,60°,90°
			Pb	8x8x8 cm	30°,60°,90°
	^{12}C	2 GeV A	C	24.25 mm	30°,60°,90°
			Al	17.21 mm	30°,60°,90°
			Cu	15.60 mm	30°,60°,90°
			Cd	12.00 mm	30°,60°,90°
			Pb	12.00 mm	30°,60°,90°
			Pb	8x8x8 mm	30°,60°,90°
8	p	2.00 GeV	Al	17.21 mm	30°,60°,90°,120°
			Cu	15.60 mm	30°,60°,90°,120°
			Cd	12.00 mm	30°,60°,90°,120°
			Pb	12.00 mm	30°,60°,90°,120°
			Pb	8x8x8 cm	30°,60°,90°,120°

* - natural mixture of isotopes
** - effective thickness along beam axis

RESULTS AND DISCUSSION

A transformation of hadron spectra with the variation of angle, target size and atomic mass of incident ion was studied in our experimental data analysis. For the proton beam a calculation of neutron distributions was also carried out by the code SITHA[16]. This computer code simulated a secondary hadrons transport using EVAP and D2N2 approximations[17] of characteristics of emitted particles in hadron-nucleus inelastic interactions.

The high-energy tail of neutron spectrum and spectra of hydrogen isotopes nuclei at 30° measured on 1 GeV·A ^{12}C ion beam with lead target 8x8x12 cm^3 are given in fig. 6. The yield of high-energy neutrons exceeds the proton yield more than by an order and the neutron spectrum overlaps very wide energy region (more than the beam ion energy per nucleon). A comparison of experimental results for high-energy neutron, proton and pion emission at angle 90° from thick lead targets bombarded by 2.55 GeV protons are shown in fig. 7. The yield of charged hadrons falls with an increase of target dimensions but the neutron yield rises.

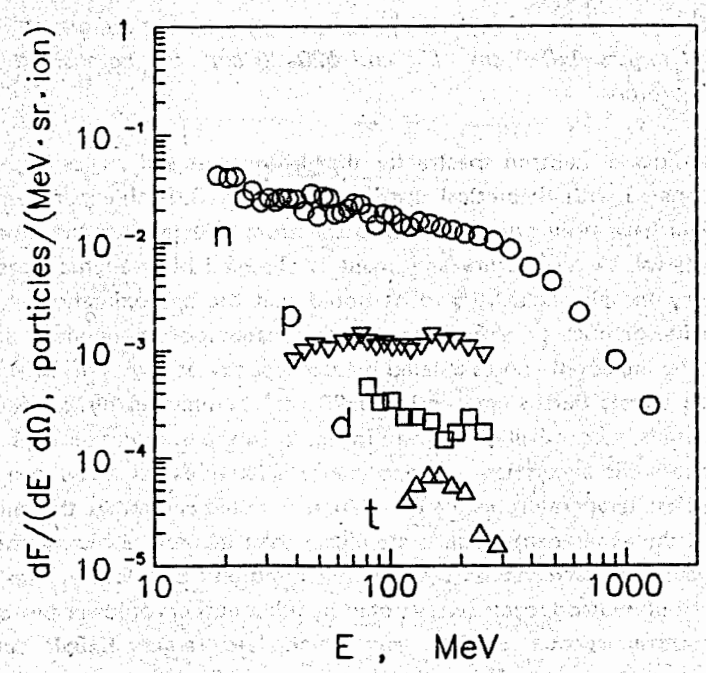

Fig. 6. Energy spectra of n, p, d and t at 30° for lead target 8x8x12 cm^3 bombarded by 1 GeV/N ^{12}C ions.

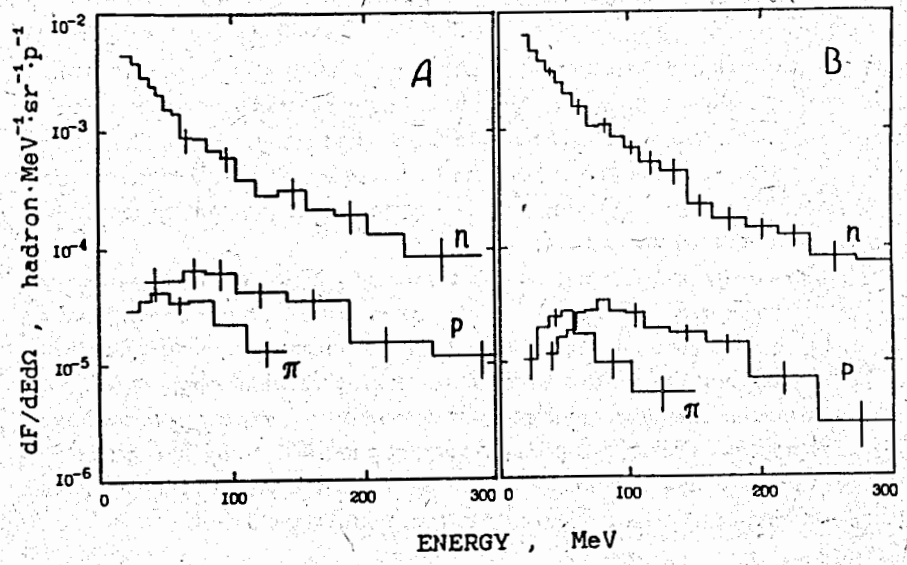

Fig. 7. Energy spectra of high-energy neutrons, protons and pions at 90° from lead targets 8x8x8 cm³ (A) and ϕ20x20 cm³ (B) bombarded by 2.55 GeV protons.

The experimental neutron spectra for thin lead target and angles 30, 90, and 150° are compared with theoretical distributions in fig. 8. Both experimental and theoretical data have been normalized on a spectrum integral over the experimental energy interval. A satisfactory argeement is observed between the experiment and the theory for all angles. It's to be noted that the approximations[17] give more high value of nuclear temperature for the evaporation component than the experiment. The measured and calculated neutron spectra at angles of 30 and 150° for thick lead targets 8x8x8 cm³ and ϕ20x20 cm³ bombarded by 2.0 GeV. and 2.55 GeV protons, respectively, are given in fig. 9. In the evaporation region a discrepancy between the experiment and the theory is likely explained by using a high value of a nuclear temperature in the calculation as noted earlier. At the same time for all targets the experimental points are higher than theoretical histograms above 20 MeV. Analogous discrepancies between measured and calculated values of the high energy tail of neutron spectra were noted by other authors at lower proton energies. The neutron spectra at 90° from thick lead targets 8x8x8 cm³ and ϕ20x20 cm³ bombarded by different ions are shown in fig. 10. All spectra have a similar shape. For incident protons the results of calculation are shown too. This experimental results are preliminary and at present the data analysis is performed.

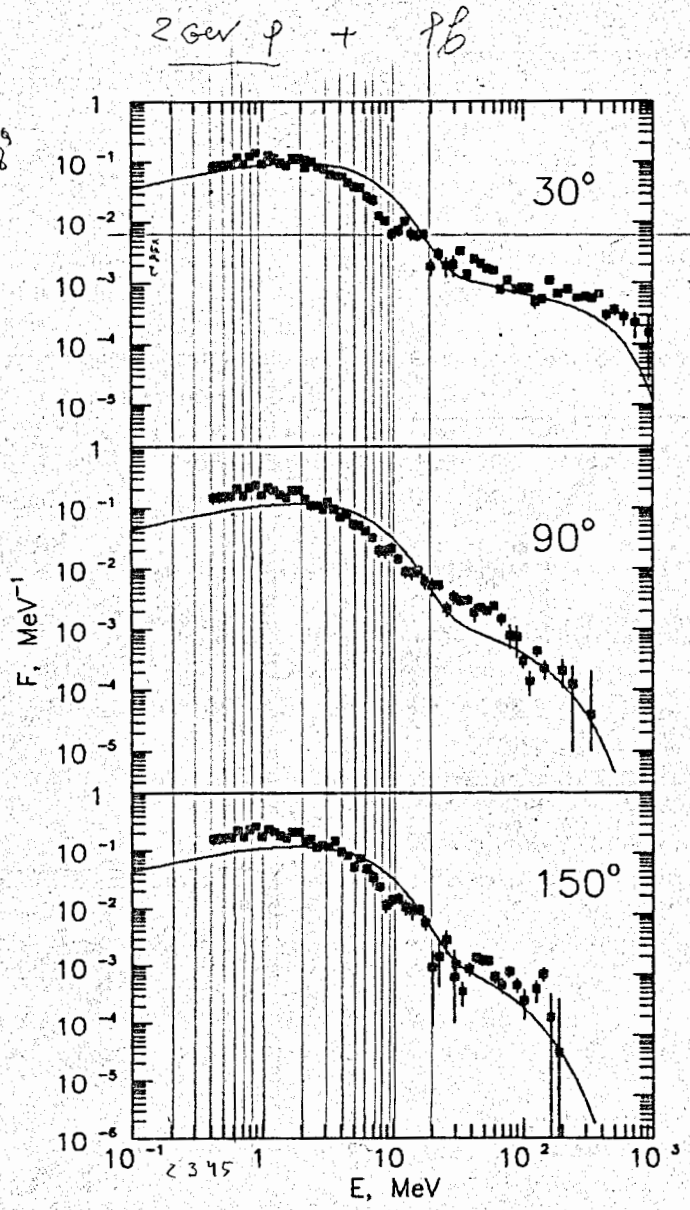

Fig. 8. Normalized neutron energy spectra for thin lead target bombarded by 2 GeV protons: points — the experiment, histograms — the calculation.

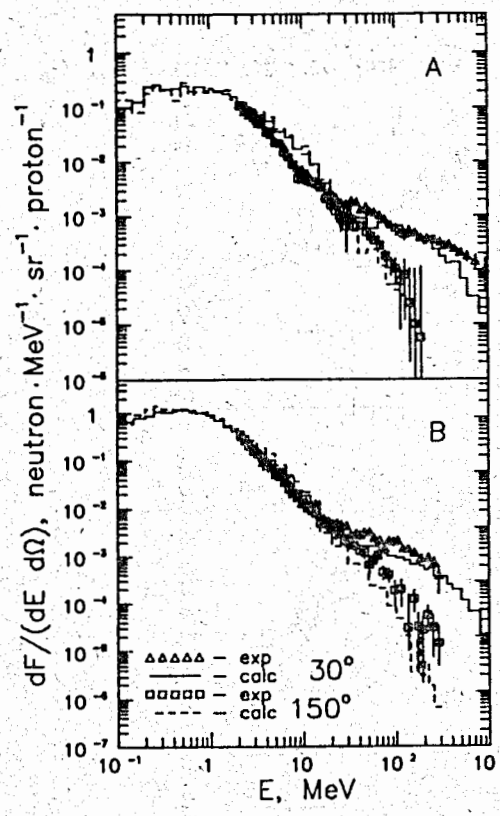

Fig. 9. Neutron spectra at 30° and 150° for lead targets 8x8x8 cm^3 (A) and ϕ20x20 cm^3 (B) bombarded by 2 GeV and 2.55 GeV protons respectively: points — the experiment, histograms — the calculation.

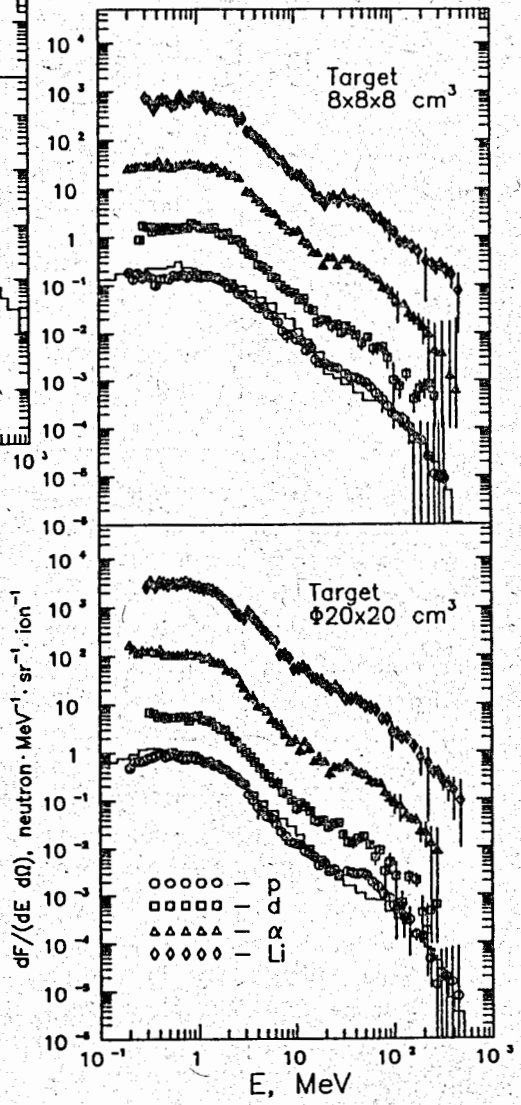

Fig. 10. Neutron spectra at 90° for lead targets 8x8x8 cm^3 and ϕ20x20 cm^3 bombarded by protons and 1 GeV·A d, α, and ^6Li ions: points — the experiment, the histogram — the calculation for a proton beam. The values for d, α and ^6Li ions have been increased by factors of 10, 100 and 1000, respectively.

REFERENCES

1. Pearlstein S. - Astrophys.J., 1989, v.346, p.1049.
2. Filges D., Armstrong T.W., Cloth P. – ICANS-VII, 1983, AECL, AECL-8488, 1983, p.194.
3. Fildes D., Cloth P., Armstrong T.W. et al. – Phys.Rev., 1987, v.C36, p.1988.
4. Ishibashi K., Takada H., Sakae T. et al. – Nuclear Data for Science and Technology. 1988 Mito, JAERI, 1988, p.1143.
5. Cierjacks S., Rainbow M.T., Swinboe M.T., Buth L. – Conf. on Neutron Physics, 1980, Kiev, M.: Atominform, 1980, Path I, p.269.
6. Cierjacks S. Raupp F., Howe S.D. et al. – ICANS-V, 1981, Julich, 1981, p.215.
7. Cierjacks S., Hino Y., Raupp F. et al. – Phys.Rev., 1987, C36, p.1976.
8. Meier M.M., Clark D.A., Goulding C.A. et al. – Nucl. Sci. and Eng., 1989, v.102, p.310.
9. Meier M.M., Goulding C.A., Morgan G.L., and Ullmann J.L. – Nucl. Sci. and Eng., 1990, v.104, p.339.
10. Amian W. Cloth P., Dragovitsch P. et al. – Nuclear Data for Science and Technology, 1991, Julich, KFA Julich (Book of Abstracts), 1991, p.116.
11. Baukov Yu.D. Gavrilov V.B., Goryainov N.A. et al. – Preprint ITEP-172, M., 1983.
12. Baukov Yu.D., Gavrilov V.B., Goryainov N.A. et al. – Preprint ITEP-148, M., 1983.
13. Cecil R.A., Anderson B.D., Baldwin A.R. et al. – Phys.Rev., 1980, v.C21, p.2471.
14. Lyapin V.G., Tsvetkov I.O., Yurevich V.I., Yakovlev R.M. – Preprint RI-217, M.: Atominform, 1990.
15. Kirillov A.D., Lyapin V.G., Rukoyatkin P.A. et al. – Report JINR P13-90-193, Dubna, 1990.
16. Daniel V.A. – Preprint RI-181, M.: Atominform, 1984.
17. Sychev B.S., Serov A.Ya. and Man'ko B.V. – Preprint RTI-799, M., 1979.

Received by Publishing Department
on April 16, 1992.